Jñānābha, Vol. 49(2) (2019), 94-104

SLIP EFFECT ON MHD STAGNATION POINT FLOW AND HEAT TRANSFER OF CROSS FLUID WITH HEAT GENERATION IN A POROUS MEDIUM

By

Navin Kumar, R. N. Jat and Sushila Choudhary

Department of Mathematics, University of Rajasthan, Jaipur-302004, India

Email:yadavnavin35@gmail.com, jat.ramniwas@gmail.com, sushilachoudhary1111@gmail.com

(*Received : November* 03*,* 2019 *; Revised: November* 07*,* 2019)

Abstract

Aim of this paper is to investigate the slip effect on magnetohydrodynamics (MHD) stagnation point flow and heat transfer of cross fluid model with heat generation in presence of porous medium. A cross fluid is a type of generalised Newtonian fluid whose viscosity depends upon shear rate according to equation (2.2). The governing nonlinear partial differential equations are transformed into ordinary differential equations along with boundary conditions by suitable similarity transformations and then reduced to a system of first order ordinary differential equations. Runge-kutta fourth order method with shooting technique is used to solve the system of first order differential equations. The effect of various physical parameters e.g. magnetic parameter, ratio parameter, Prandtl number, Weissenberg number, permeability parameter, heat source/sink parameter on velocity, temperature, skin friction and Nusselt number are presented through graphs, table and discussed numerically.

2010 Mathematics Subject Classification: 76D05, 76D10, 76E25, 76S05, 76W05, 80A20.

Keywords and phrases: Heat transfer, MHD, Stagnation point flow, Cross fluid model, Slip condition, Heat generation, porous medium.

1 Introduction

Firstly the steady of behaviour of boundary layer flow of incompressible fluid due to a stretching surface was analyzed by Crane [5]. Ishak et al. [7] analysed the steady two-dimensional stagnation-point mixed convection flow of an incompressible viscous fluid towards a stretching vertical permeable sheet in its own plane. The stretching velocity and the surface temperature are assumed to vary linearly with the distance from the stagnation-point. Rashad et al. [12] have studied the effect of uniform transpiration velocity on free convection boundary-layer flow of a non-Newtonian fluid over a permeable vertical cone embedded in a porous medium saturated with a nanofluid. Bhattacharyya et al. [2] obtained the solutions of boundary layer flow and heat transfer for two classes of viscoelastic fluid over a stretching sheet with internal heat generation or absorption. A numerical study of the slip effect on the unsteady mixed convection boundary-layer flow near the two-dimensional stagnation point on a vertical permeable surface embedded in a fluid-saturated porous medium with suction has been carried out by Rohni et al. [13]. Effect of thermal radiation on the flow of micropolar fluid and heat transfer past a porous shrinking sheet has been investigated by Bhattacharyya et al. [3]. Bhattacharyya et al. [4] have analyzed

the steady boundary layer slip flow and mass transfer over a porous plate embedded in a Darcy porous medium. Makinde [9] has considered the hydromagnetic mixed convection stagnation point flow towards a vertical plate embedded in a highly porous medium with radiation and internal heat generation. Akbar et al. [1] have considered the two-dimensional stagnation-point flow of an incompressible Carreau fluid towards a shrinking surface with dual solutions. Two dimensional boundary layer flow and the heat transfer of a Maxwell fluid past a stretching sheet are studied numerically by Nadeem et al. [10]. Li et al. [8] have analyzed MHD viscoelastic flow due to a vertical stretched surface with Cattaneo-Christov heat flux. Stagnation point flow of Maxwell fluid towards a permeable stretching sheet in the presence of nano particles has been studied by Ramesh et al. [11]. Sharma et al. [14] have discussed MHD slip flow and heat transfer over an exponentially stretching perameable sheet embedded in a porous medium in the presence of heat source. Hayat et al. [6] have analyzed the heat transfer in MHD stagnation point flow of cross fluid model in the presence of magnetic fluid due to stretching sheet. MHD stagnation point flow and heat transfer of a Williamson fluid in the direction of an exponentially stretching sheet embedded in a thermally stratified medium subject to suction is discussed by Vittal et al. [15].

Our main aim in this paper is to investigate of MHD stagnation point flow of cross fluid along stretched surface surface in the presence of porous medium. The slip conditions are imposed on both velocity and temperature. After using similarity transformations, reduced non linear ODE's are solved numerically with shooting technique. The Runge-kutta scheme of fourth order is used for integration. The effects of pertinent parameters on velocity and temperature profiles are discussed in result section.

2 Formulation of the Problem

Consider the steady MHD stagnation point flow of cross fluid with heat generation in the presence of porous medium over an stretched surface. The Cauchy stress tensor τ of a cross fluid model is expressed as

$$\tau = -pI + \mu A_1 \tag{2.1}$$

where p is the pressure, I is the identity matrix, A_1 is the first Rivlin-Erickson tensor and μ is the viscosity of cross fluid model. The viscosity of cross fluid in terms of shear rate is given as

$$\mu = \mu_\infty + (\mu_0 - \mu_\infty)\left[\frac{1}{1 + (\Gamma\dot{\gamma})^{1-n}}\right] \tag{2.2}$$

or

$$\frac{\mu_0 - \mu}{\mu - \mu_\infty} = (\Gamma\dot{\gamma})^{1-n}, \tag{2.3}$$

where μ_0 is the zero shear rate viscosity, μ_∞ is the infinite shear rate viscosity, Γ is the cross time constant and n is the power law index. The shear rate $\dot{\gamma}$ is defined as

$$\dot{\gamma} = \left[4\left(\frac{\partial u}{\partial x}\right)^2 + \left(\frac{\partial u}{\partial y} + \frac{\partial u}{\partial x}\right)^2\right]^{\frac{1}{2}}. \tag{2.4}$$

The first Rivlin-Erickson tensor A_1 is given by

$$A_1 = \dot{L} + \dot{L}^T, \tag{2.5}$$

where $\dot{L}$ is velocity gradient.

Flow equation of momentum and heat transfer for cross fluid model after applying the boundary layer approximation can be written as

$$\frac{\partial u}{\partial x}+\frac{\partial v}{\partial y}=0, \tag{2.6}$$

$$u\frac{\partial u}{\partial x}+v\frac{\partial u}{\partial y}=v\frac{\partial}{\partial y}\left[\frac{\frac{\partial u}{\partial y}}{1+\left\{\Gamma\left(\frac{\partial u}{\partial y}\right)\right\}^{1-n}}\right]+u_e\frac{dU_e}{dx}+\frac{v}{k}(u_e-u)+\frac{\sigma B_0}{\rho}(u_e-u), \tag{2.7}$$

$$u\frac{\partial T}{\partial x}+v\frac{\partial T}{\partial y}=\alpha\frac{\partial^2 T}{\partial y^2}+\frac{Q_0}{\rho c_p}\left(T-T_\infty\right), \tag{2.8}$$

where u and v are the velocity components along the x and y-axes respectively, t is time, α is the thermal diffusivity, υ is the kinematic viscosity, ρ is the density of fluid, k is the permeability of the porous medium, T is the temperature of the fluid within the boundary layer and T_∞ is the temperature of fluid outside the boundary layer, Q_0 is the heat generation coefficient .

The boundary conditions are

$$\left.\begin{array}{l} u=u_w=c_1x+L\frac{\partial u}{\partial y}, v=0, T=T_w+L'\frac{\partial T}{\partial y} aty=0 \\ u\to u_e=c_2x, T\to T_\infty asy\to\infty \end{array}\right\}. \tag{2.9}$$

3 Method of Solution

Introducing the following transformations, functions and dimensionless quantities

$$\left.\begin{array}{l} \eta=\sqrt{\frac{c_1}{\upsilon}}y, \psi=\sqrt{c_1\upsilon}xf(\eta), \theta(\eta)=\frac{T-T_\infty}{T_w-T_\infty}, \\ u=\frac{\partial\psi}{\partial y}, v=-\frac{\partial\psi}{\partial x}, A=\frac{c_2}{c_1}, K=\frac{\upsilon}{kc_1}, \mathrm{Pr}=\frac{\upsilon}{\alpha}, \\ We=c_1\Gamma Re^{\frac{1}{2}}, M=\frac{\sigma B_0^2}{\rho c_1}, \delta=\frac{Q_0}{\rho c_p c_1} \end{array}\right\}, \tag{3.1}$$

into equation (2.6) to (2.8), we get

$$\left(ff''-f'^2\right)\left[1+(Wef'')^{1-n}\right]^2+\left[A^2+(M+K)(A-f')\right]\left[1+(Wef'')^{1-n}\right]^2 + \left[1+n(Wef'')^{1-n}\right]f'''=0, \tag{3.2}$$

$$\frac{1}{\mathrm{Pr}}\theta''+f\theta'+\delta\theta=0, \tag{3.3}$$

where prime denotes the differentiation with respect to η, A is the velocity ratio parameter, M is magnetic parameter, Pr is Prandtl Number, We is the Weissenberg number, $K$is the permeability parameter,δ is heat source/sink parameter.

It is noted that the equation of continuity (2.6) is identically satisfied.

The corresponding boundary conditions are reduced to

$$\left.\begin{array}{l} f(0)=0, f'(0)=1+Lvf''(0), \theta(0)=1+Lt\theta'(0) at\eta=0 \\ f'(\infty)=A, \theta(\infty)=0 at\eta=\infty \end{array}\right\}, \tag{3.4}$$

where $Lv=L\sqrt{\frac{c_1}{\upsilon}}$ and $Lt=L'\sqrt{\frac{c_1}{\upsilon}}$ is the slip parameter.

The physical quantities of interest are the local skin-friction coefficientC_f, heat transfer rate i.e. the local Nusselt number Nu_x, and their mathematical expressions are as follows

$$C_f=\frac{\tau_w}{\frac{1}{2}\rho U_w^2}, Nu_x=\frac{q_w x}{k(T_w-T_\infty)}, \tag{3.5}$$

where the wall shear stress τ_w and the heat flux q_w are given by

$$\tau_w = \left[\mu_0 \frac{\frac{\partial u}{\partial y}}{1 + \left\{ \Gamma \left(\frac{\partial u}{\partial y} \right) \right\}^{1-n}} \right]_{y=0}, q_w = -k \left(\frac{\partial T}{\partial y} \right)_{y=0}, \tag{3.6}$$

Using the similarity transformation given in equation (3.1), we get the following expression

$$\frac{1}{2} C_f Re_x^{1/2} = \frac{f''(0)}{1 + (We f''(0))^{1-n}}, Nu_x Re_x^{-1/2} = -\theta'(0). \tag{3.7}$$

where $Re_x = \frac{U_w^2}{c_1 \upsilon}$ is the local Reynolds number.

The set of equation (3.2) and (3.3) subject to the boundary condition (3.4) are solved numerically using the Runge-Kutta fourth order method with shooting technique. Equations (3.2) and (3.3) are transformed into system of first order differential equations as given below

$$\left.\begin{aligned} f_1' &= f_2, \\ f_2' &= f_3, \\ f_3' &= -\frac{\left[1+(We f_3)^{1-n}\right]^2}{\left[1+n(We f_3)^{1-n}\right]} \left[f_1 f_3 - f_2^2 + A^2 + (M+K)(A - f_2) \right], \\ f_4' &= f_5, \\ f_5' &= -\Pr \left(f_1 f_5 + \delta f_5 \right), \end{aligned}\right\} \tag{3.8}$$

where $f = f_1, f' = f_2, f'' = f_3, f''' = f_3', \theta = f_4, \theta' = f_5, \theta'' = f_5'$ subject to the following conditions

$$\left.\begin{aligned} &f_1(0) = 0, f_2(0) = 1 + Lv f_3(0), f_4(0) = 1 + Lt f_5(0) \\ &f_2(\infty) = A, f_4(\infty) = 0. \end{aligned}\right\}. \tag{3.9}$$

In order to get solution, values of $f_3(0)$ and $f_5(0)$ i.e. $f''(0)$ and $\theta'(0)$ are required, but no such values are given in the boundary conditions, therefore according to shooting technique initial guesses for $f_3(0)$ and $f_5(0)$ are taken as $s_1 and s_2$, respectively. Then we compare the calculated values for f_2, f_4 at η_∞ (a suitable gauss ofη) with the given boundary conditions $f_2(\eta_\infty = 4) = 0, f_4(\eta_\infty = 10) = 0$ and adjust the estimated values of$f''(0)$ and $\theta'(0)$ using the Secant method to give a better approximation for the solution. The step-size is taken $h = 0.002$. The above procedure is repeated until we get the converged results within a tolerance limit of 10^{-3}. All the computations are carried out on Matlab software.

4 Results and Discussion

The behaviour of A, which denotes the ratio of free stream velocity to the velocity of the stretching sheet on the velocity field can be observed from Fig. 4.1. The velocity of the fluid and the boundary layer thickness increases when free stream velocity is less than the velocity of the stretching sheet $A < 1$ with an increase in A. However when free stream velocity exceeds the velocity of the stretching sheet $A > 1$, the velocity of the fluid increases where as the boundary layer thickness decreases with an increase in A.

Now, we see the influence of the permeability parameter K on the velocity profiles. Fig. 4.2 shows the variation in velocity field for several values of K. With increase of K the dimensionless velocity $f'(\eta)$ along the plate decreases and consequently the momentum boundary layer thickness decreases. This is due to physical fact that resistance diminishes as permeability of the medium increases. So progressively less drag is experienced by the flow and flow retardation is thereby decreased. Thus the permeability parameter enhances the fluid motion inside the boundary layer.

The effect of magnetic parameter M on velocity profiles are shown by Fig. 4.3. It is observed that the fluid velocity decreases as the values of M increases. This leads to the fact that rate of transport decreases with the increment in M because the Lorentz force which opposes the motion of fluid increases with the increment in M.

Fig. 4.4 illustrates the influence of Weissenberg number We on velocity profiles. It shows that velocity increases as Weissenberg number increases.

The effect of velocity slip parameter on fluid velocity is presented by Fig. 4.5. It is observed that fluid velocity decreases as velocity slip parameter increases.

The influence of heat source ($\delta > 0$) parameter on the dimensionless temperature profiles is illustrated by Fig. 4.6. Due to increase in the strength of the heat source the fluid temperature increases as the thermal boundary layer thickness enlarges.

Fig. 4.7 represented the effect of Prandtl number on the temperature profiles. Beyond the surface the value of the temperature as well as thermal boundary layer thickness rapidly decrease with increasing Pr but near the surface the results are reverse. An increase in Prandtl number means an increase of fluid viscosity which causes a decrease in the flow velocity and the temperature decreases. This is also consistent with the fact that the thermal boundary layer thickness decreases with increasing Prandtl number.

The effect of temperature slip parameter on fluid temperature is shown by Fig. 4.8. It is observed that as the temperature slip parameter increases, fluid temperature decreases.

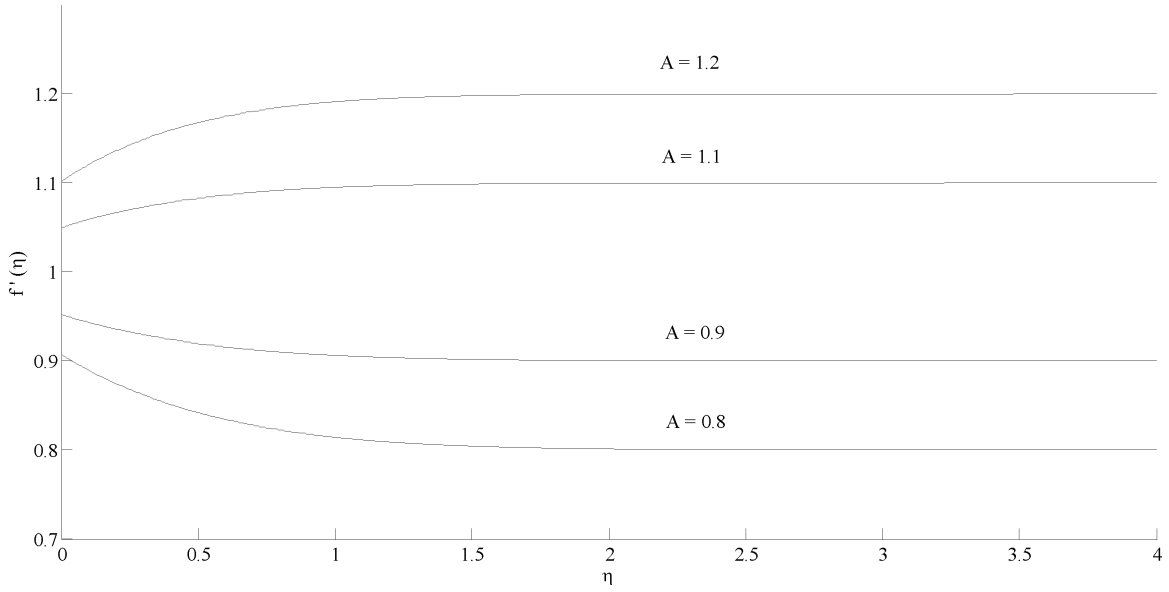

Figure 4.1: Velocity profile against η for various values of ratio parameter A when K=1.0, $M = 0.09$, Pr $= 1.2$, $We = 0.2$, $\delta = 1.0$, $Lv = 0.5$, $Lt = 0.5$ and $m = 0.1$

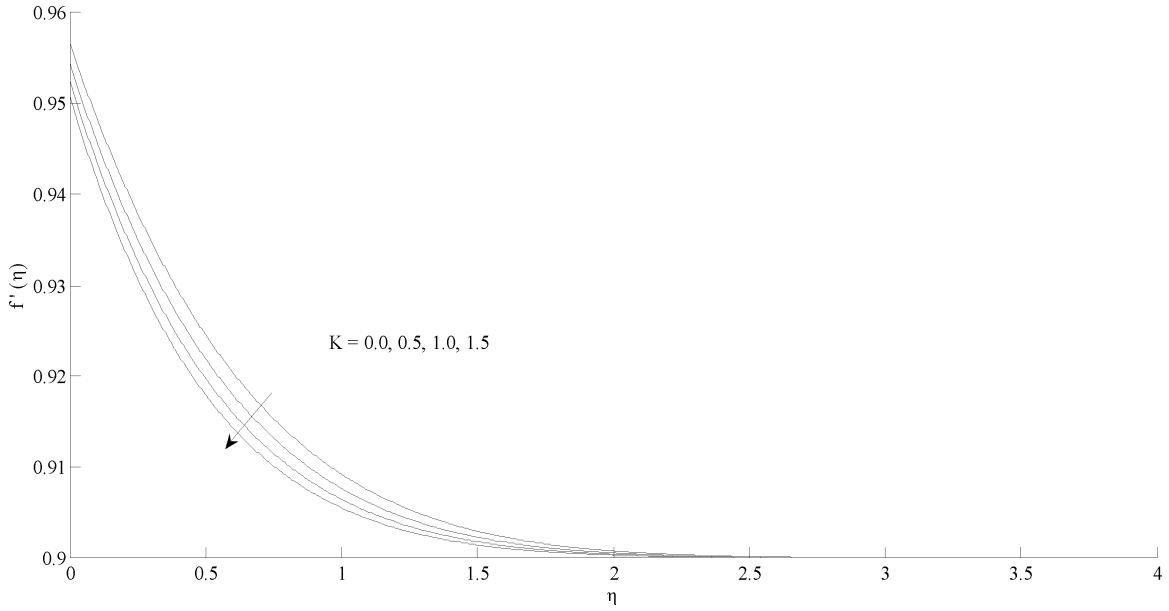

Figure 4.2: Velocity profile against η for various values of K when $M = 0.09$, $A = 0.9$, Pr $= 1.2$, $We = 0.2$, $\delta = 1.0$, $Lv = 0.5$, $Lt = 0.5$ and $m = 0.1$.

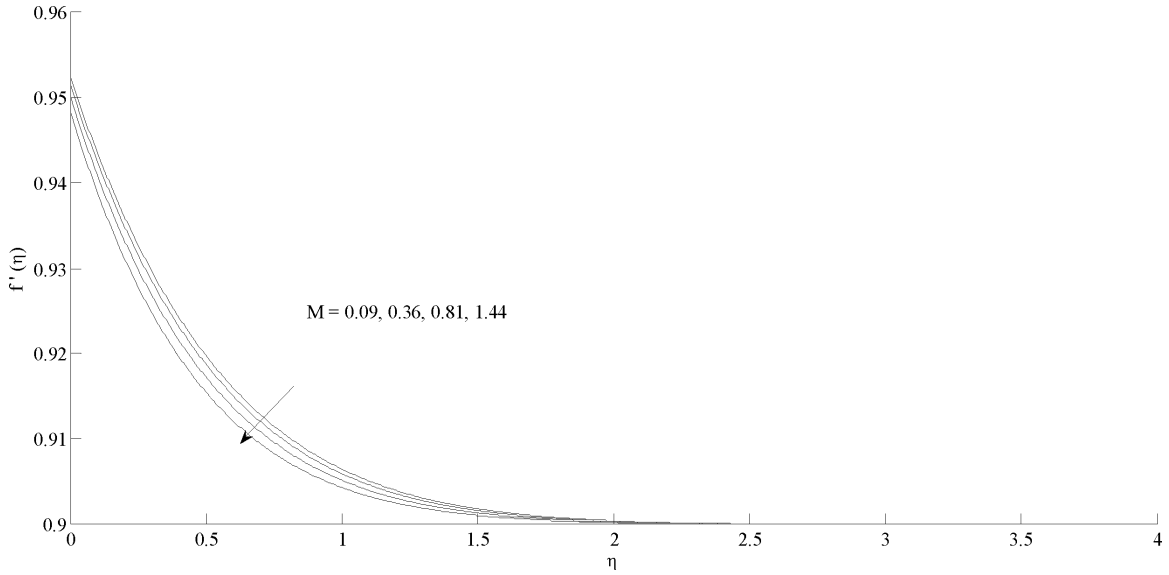

Figure 4.3: Velocity profile against η for various values of Magnetic Parameter M when K=1.0, $A = 0.9$, Pr $= 1.2$, $We = 0.2$, $\delta = 1.0$, $Lv = 0.5$, $Lt = 0.5$ and $m = 0.1$.

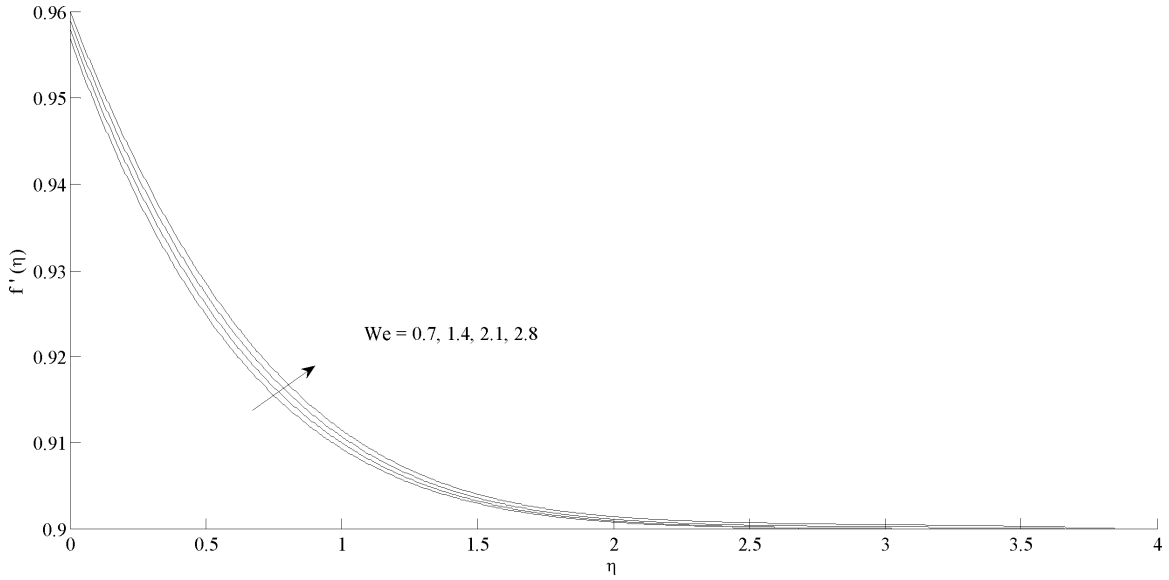

Figure 4.4: Velocity profile against η for various values of Weissenberg Number We when K=0.1, $M = 0.09$,$A = 0.9$, Pr $= 1.2$, $\delta = 1.0$, $Lv = 0.5$, $Lt = 0.5$ and $m = 0.1$.

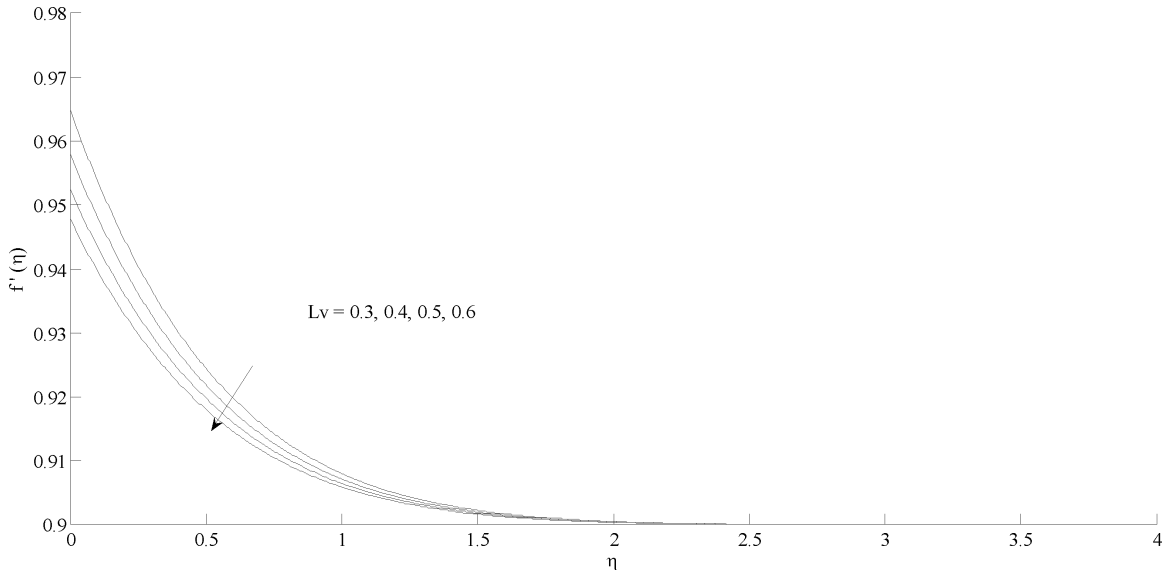

Figure 4.5: Velocity profile against η for various values of Lv when K=1.0, $M = 0.09$, $A = 0.9$, Pr $= 1.2$, $We = 0.2$, $\delta = 1.0$, $Lt = 0.5$ and $m = 0.1$.

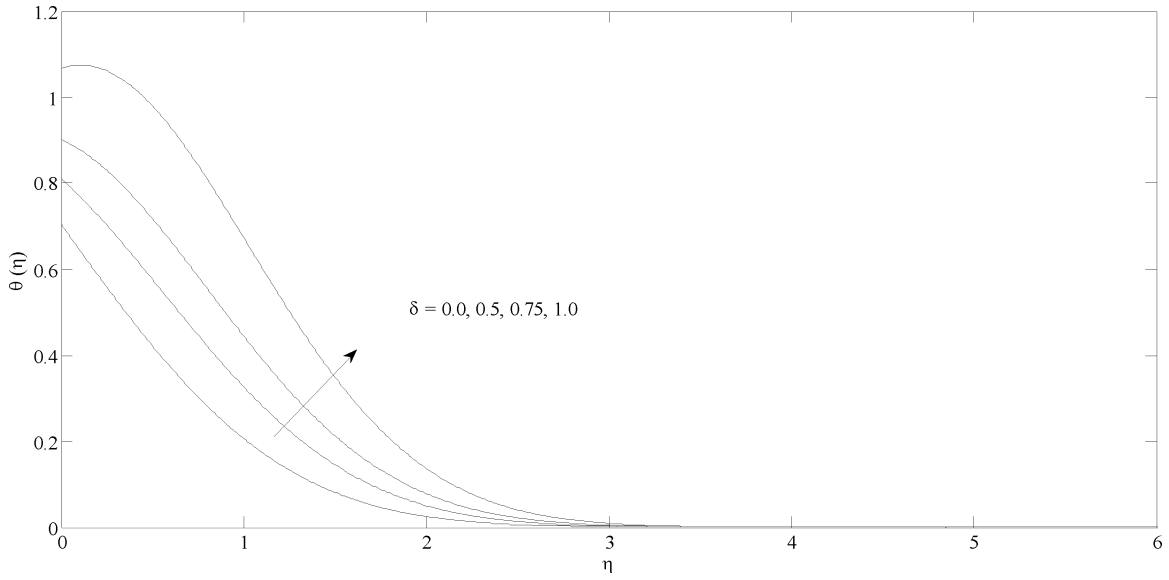

Figure 4.6: Temperature profile against η for various values of δ when K=1.0, $M = 0.09$, $A = 0.9$, $We = 0.2$, Pr $= 1.2$, $Lv = 0.5$, $Lt = 0.5$ and $m = 0.1$.

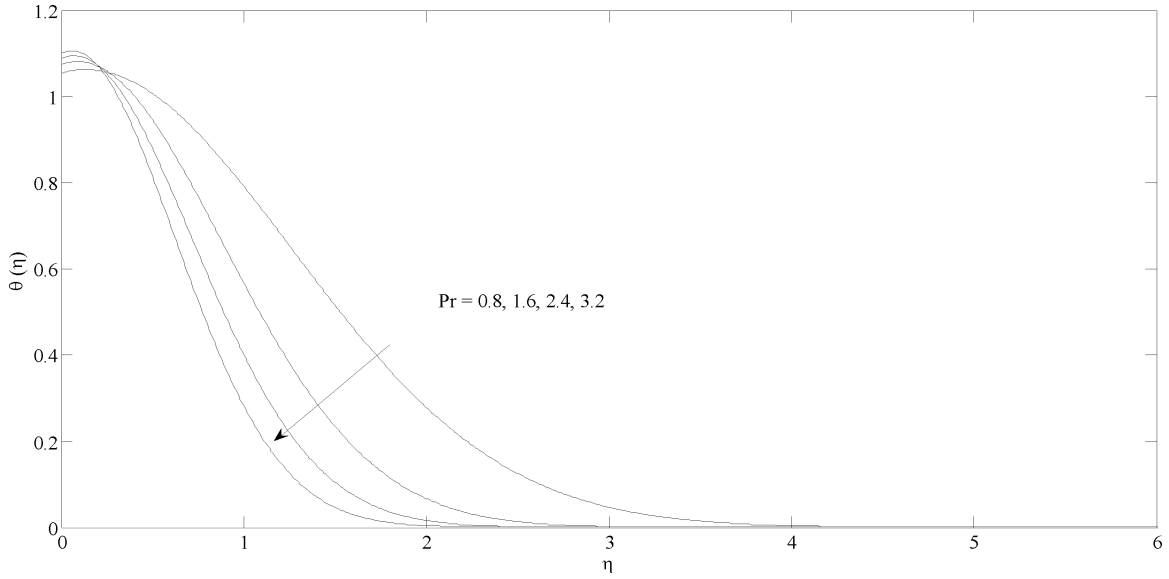

Figure 4.7: Temperature profile against η for various values of Prandtl Number Pr when K=1.0, $M = 0.09$, $A = 0.9$, $We = 0.2$, $\delta = 1.0$, $Lv = 0.5$, $Lt = 0.5$ and $m = 0.1$.

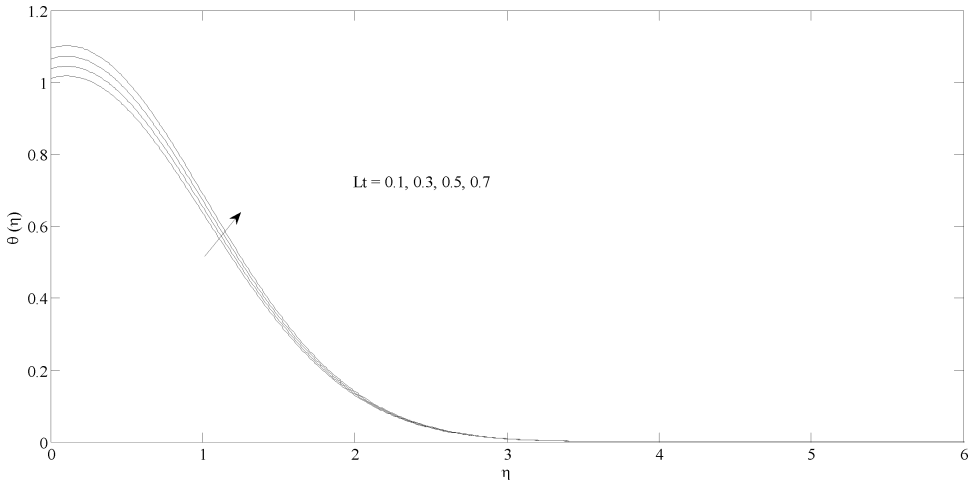

Figure 4.8: Temperature profile against η for various values of Lt when K=1.0, $M = 0.09$, $A = 0.9$, $We = 0.2$, Pr $= 1.2$, $\delta = 1.0$, $Lv = 0.5$ and $m = 0.1$.

Table 4.1: Numerical values of skin friction coefficient $\{-f''(0)\}$ and local Nusselt number $\{-\theta'(0)\}$ for various values of physical parameters.

A	M	K	We	Lv	Pr	δ	Lt	$-f''(0)$	$-\theta'(0)$
0.8	0.09	1.0	0.2	0.5	1.2	1.0	0.5	0.1859886	-0.13665
0.9								0.0952272	-0.13361
1.1								-0.0998319	0.09788
1.2								-0.2039279	0.17381
0.9	**0.09**							0.0952272	-0.13361
	0.36							0.0970852	-0.13506
	0.81							0.0999093	-0.13719
	1.44							0.1033948	-0.13972
	0.09	**0.0**						0.0868974	-0.12675
		0.5						0.0913896	-0.13052
		1.0						0.0952272	-0.13361
		1.5						0.0985679	-0.13619
		0.1	**0.7**					0.0933752	-0.13232
			1.4					0.0909191	-0.13034
			2.1					0.0884658	-0.12799
			2.8					0.0859435	-0.12508
		1.0	0.2	**0.3**				0.0861875	-0.12629
				0.4				0.0840204	-0.12461
				0.5				0.0819309	-0.12280
				0.6				0.0798756	-0.12095
				0.5	**0.8**			0.0952223	-0.11292
					1.6			0.0952223	-0.15249
					2.4			0.0952223	-0.18125
					3.2			0.0952223	-0.20481
					1.2	**0.0**		0.0952223	0.59195
						0.5		0.0952223	0.37973
						0.75		0.0952223	0.19536
						1.0		0.0952223	-0.13575
						1.0	**0.1**	0.0952223	-0.12786
							0.3	0.0952223	-0.13121
							0.5	0.0952223	-0.13475
							0.7	0.0952223	-0.13848

5 Conclusions

In this paper we have studied slip effect on MHD stagnation point flow and heat transfer of Cross fluid in presence of porous medium. The main findings of this study are as follows:

1. It is observed that velocity decreases as permeability parameter or magnetic parameter increases.
2. Velocity increases as Weisenbreg number increases.
3. Increment in velocity slip parameter and temperature slip parameter enhance both, velocity and temperature profiles.
4. Thermal boundary layer increases as heat source parameter δ increases.
5. The drag force decreases as parameter A increases while it increases as magnetic parameter$M$, permeability parameter K increases. The Nusselt number $(-\theta'(0))$ decreases as temperature slip parameter increases.

Acknowlegement

We are very much thankful to the referee for his valuable suggestions to bring the paper in its present form.

References

[1] N. S. Akbar, S. Nadeem, R. U. Haq and Shiwei Ye, MHD stagnation point flow of Carreau fluid towards a permeable shrinking sheet, Dual solutions, *Ain Shams Engineering Journal*, **5** (2014), 1233-1239.

[2] K. Bhattacharyya, M. S. Uddin, G. C. Layek and W. Ali Pk, Analysis of boundary layer flow and heat transfer for two classes of viscoelastic fluid over a stretching sheet with heat generation or absorption, *Bangladesh J. Sci. Ind. Res.,* **46(4)** (2011), 451-456.

[3] K. Bhattacharyya, S. Mukhopadhyay, G.C. Layek and I. Pop, Effects of thermal radiation on micropolar fluid flow and heat transfer over a porous shrinking sheet, *International Journal of Heat and Mass Transfer*, **55** (2012), 2945-2952.

[4] K. Bhattacharyya, slip effects on boundary layer flow and mass transfer with chemical reaction over a permeable flat plate in a porous medium, *Frontiers in Heat and Mass Transfer (FHMT)*, **3** (2012).

[5] L. J. Crane, Flow past a stretching plate, *J. Appl. Math. Phy.*, **21(4)** (1970), 645-647.

[6] T. Hayat, M. I. Khan, M. Tamoor, M. Waqas and A. Alsaedi, Numerical simulation of heat transfer in MHD stagnation point flow of Cross fluid model towards a stretched surface, *Result in Physics*, **7** (2017), 1824-1827.

[7] A. Ishak, R. Nazar, N. M. Arifin and I. Pop, Mixed convection of the stagnation-point flow towards a Stretching vertical permeable sheet, *Malaysian Journal of Mathematical Sciences*, **1(2)** (2007), 217-226.

[8] J. Li, L. Zheng and L. Liu, MHD viscoelastic flow and heat transfer over a vertical stretching sheet with Cattaneo-Christov heat flux effects, *J. Mol. Liq.,* **221** (2016), 19-25.

[9] O. D. Makinde, Heat and mass transfer by MHD mixed convection stagnation point flow toward a vertical plate embedded in a highly porous medium with radiation and internal heat generation, *Meccanica*, **47** (2012), 1173-1184

[10] S. Nadeem, R. Ul Haq and Z. H. Khan, Numerical study of MHD boundary layer flow of a Maxwell fluid past a stretching sheet in the presence of nanoparticles, *J. Taiwan Inst Chem Eng.*, **45(1)** (2014), 121-126.

[11] G. K. Ramesh, B. J. Gireesha, T. Hayat and A. Alsaedi, Stagnation point flow of Maxwell fluid towards a permeable surface in the presence of nanoparticles, *Alex Eng J.*, **55(2)** (2016), 857-65.

[12] A. M. Rashad, M. A. EL-Hakiem and M. M. M. Abdou, Natural convection boundary layer of a non-Newtonian fluid about a permeable vertical cone embedded in a porous medium saturated with a nanofluid, *Computers and Mathematics with Applications*, **62** (2011), 3140-51.

[13] A. M. Rohni, S. Ahmad, I. Pop and J. H. Merkin, Unsteady mixed convection boundary-layer flow with suction and temperature slip effects near the stagnation point on a vertical permeable surface embedded in a porous medium, *Transp Porous Med.*, **92** (2012), 1-14.

[14] P. R. Sharma, S. Choudhary and O. D. Makinde, MHD slip flow and heat transfer over an exponentially stretching permeable sheet embedded in porous medium with heat source, *Frontiers in Heat and Mass Transfer*, **9(8)** (2017).

[15] C. Vittal, M. C. K. Reddy and T. Vijayalaxmi, MHD stagnation point flow and heat transfer of Williamson fluid over exponential stretching sheet embedded in a thermally stratified medium, *Global Journal of Pure and Applied Mathematics*, **13(6)** (2017), 2033-2056.